Excitation of Pb^{206}, Pb^{207}, Pb^{208}, and Bi^{209} by Inelastic Electron Scattering*†

J. F. ZIEGLER‡ AND G. A. PETERSON§
Electron Accelerator Laboratory and Department of Physics, Yale University, New Haven, Connecticut
(Received 14 August 1967)

High-resolution measurements of the differential cross sections for inelastic scattering of 28- to 73-MeV electrons by Pb^{206}, Pb^{207}, Pb^{208}, and Bi^{209} nuclei have been analyzed by using a distorted-wave code to extract reduced nuclear radiative transition probabilities [$B(EL)$'s], and transition radii. The use of an irrotational and incompressible vibrating-liquid-drop model resulted in good fits to the data. In agreement with de-Shalit's weak-coupling core-excited state model, the $B(EL)$'s were found to be equal for the three lead isotopes within an experimental error of about 6% for the $E2$ excitations at about 4.1 MeV, and for the $E4$'s at about 4.3 MeV. For all four isotopes the $B(E3)$'s at about 2.6 MeV were equal. Excitations of Pb^{208} at 5.25 MeV (3^- or 4^+), 5.6 MeV (3^-), and 6.2 MeV (2^+ or 0^+) were observed. No strong $E2$ excitation of Pb^{208} was identified between 6.2 and 18 MeV. A discussion of model and parameter dependence of the $B(EL)$'s and transition radii is given.

I. INTRODUCTION

ALTHOUGH the purely electromagnetic excitation of nuclei by deeply penetrating high-energy electrons has promise as a means of studying the detailed structure of nuclear states,[1] the results obtained from many inelastic electron scattering experiments have been of limited accuracy. One experimental difficulty has been a lack of energy resolution and the inability to clearly separate neighboring peaks. Another difficulty has been one of analysis, because a procedure for taking into account the distortion of the incoming and outgoing electron waves by the Coulomb potential of the nucleus has not been available. Recourse to the plane-wave Born approximation has been a necessary though inadequate procedure, especially for heavy nuclei and for low-energy electrons.

We have carried out high-resolution studies of the elastic and inelastic scattering of 28- to 73-MeV electrons from Pb^{206}, Pb^{207}, Pb^{208}, and Bi^{209}. Previous methods of analysis have been improved by the use of distorted-wave codes for both the elastic and inelastic scattering. This permitted a more accurate extraction of nuclear parameters from the experimental data than would the use of the Born approximation. From another point of view, these results for heavy nuclei may be compared with results obtained by other means as a check of the entire method of analysis.

There are similarities in the analysis of elastic and inelastic scattering. For low-momentum-transfer elastic scattering, only one parameter can be extracted to give an indication of the size of the nucleus in the ground state.[2] This is the rms radius, which is related to the second radial moment of the charge distribution. As the momentum transfer q is increased, fourth and higher moments may be extracted.[3] This approach of obtaining moments of the ground-state charge distribution has not been followed in highly model-sensitive, high-q elastic scattering studies. Instead, models of charge distributions have been used in the calculation of cross sections which were compared with experiment.

For electric multipole excitation by inelastic electron scattering, the Lth radial moment of the transition charge density is related to the nuclear transition probability $B(EL)$ and the "$L+2$" radial moment to the transition radius R_{tr} as we shall expand upon in Sec. III B.[4,5] The transition radius has the same significance for the excited state as the rms radius has for the ground state. For experiments over a broad range of q, the approach of assuming a model and comparing directly a computed inelastic cross section with experiment is more appropriate than the extraction of the first few moments.

We have extracted values of both $B(EL)$ and R_{tr} through the use of the inelastic distorted-wave code of Griffy, Biedenharn, Reynolds, Onley, and Wright,[6] hereafter referred to as GBROW.[7] Tassie's[8] macroscopic nuclear model of a vibrating incompressible and irrotational liquid drop was incorporated into the code. In this model, the transition charge density is proportional to the first radial derivative of the ground-state charge density and is located at the nuclear surface.

* Part of this work was submitted by J. F. Ziegler to the faculty of Yale University in partial fulfillment of the requirements for the degree of Doctor of Philosophy.

† Work supported by the U. S. Atomic Energy Commission under contract AT 2726-503.

‡ Present address: Thomas J. Watson Research Center, IBM, Yorktown Heights, N. Y.

§ Presently on leave at Instituut voor Kernphysisch Onderzoek, Amsterdam, The Netherlands.

[1] W. C. Barber, Ann. Rev. Nucl. Sci. **12**, 1 (1962); T. DeForest, Jr., and J. D. Walecka, Advan. Phys. **15**, 1 (1966).

[2] F. Bitter and H. Feshbach, Phys. Rev. **92**, 837 (1953).

[3] L. R. B. Elton, *Nuclear Sizes* (Oxford University Press, London, 1961).

[4] R. H. Helm, Phys. Rev. **104**, 1466 (1956).

[5] G. Fricke, thesis, Darmstadt, 1962 (unpublished); E. Spamer, Z. Physik **191**, 24 (1966).

[6] T. A. Griffy, D. S. Onley, J. T. Reynolds, and L. C. Biedenharn, Phys. Rev. **128**, 883 (1962); D. S. Onley, T. A. Griffy, and J. T. Reynolds, *ibid.* **129**, 1689 (1963); D. S. Onley, J. T. Reynolds, and L. E. Wright, *ibid.* **134**, B945 (1964); D. S. Onley, L. E. Wright, and S. T. Tuan (private communications).

[7] J. Ziegler (unpublished).

[8] L. J. Tassie, Australian J. Phys. **9**, 407 (1956).

Helm[4] has used as a similar macroscopic model a Gaussian charge distribution at the nuclear surface.

A discussion of model independence of low-energy inelastic electron scattering is given in Sec. III B by contrasting the results assuming the macroscopic Tassie model with those obtained by assuming the very different microscopic Gillet random phase approximation.[9]

In another aspect we have compared the $B(EL)$'s of the collective $E2$, $E3$, and $E4$ transitions below 5 MeV for the isotopes studied. Within experimental error they are equal, as is predicted by the weak-coupling core-excited state model of de-Shalit.[10] A comparable study[11] is underway for the comparison of the excited states of Sr^{88} to those of Y^{89} treated as a $2p_{1/2}$ proton coupled to the excited states of Sr^{88}. Here agreement between theory and experiment is not found.

Preliminary reports of these experiments have been given.[12–14]

II. EXPERIMENTAL METHOD

The electron beam for these measurements was produced by the Yale University five-section, L-band, traveling-wave linear accelerator of 75-MeV peak energy and 10^{-3} duty cycle. A few μA of the accelerator beam spectrum, resolved in energy to about 2×10^{-3}, was deflected by an achromatic four-magnet system,[15] and focused on the target by a quadrupole triplet magnetic lens. The electrons scattered from the target were analyzed by a 180° double-focusing magnetic spectrometer of 16-in. central radius of curvature.[16] The beam that passed through the target was received by a Faraday cup of standard design and integrated by a commercial current integrator. The electrons passed through vacuum foils only at the output of the spectrometer where they were detected by four counter telescopes using plastic scintillators in coincidence. Nanosecond circuitry was necessary because of the low duty cycle, high elastic peak counting rates, and high backgrounds. A more complete description of this equipment will be published in another article.[17] The over-all absolute resolution obtained with this equipment was nearly an order of magnitude better than that of an earlier experiment[18] on Pb and Bi.

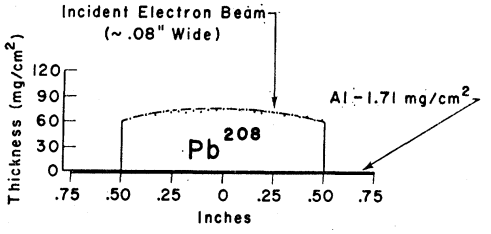

FIG. 1. Radial distribution of Pb^{208} target on Al backing.

In order to obtain well-defined peaks it was necessary to use a beam spot on target of approximately 2 mm×2 mm. The high current densities resulted in target heating problems for the low-melting-point targets of this work. Therefore it was necessary to evaporate the target metals on 0.17-mg cm^{-2} aluminum foils and then rotate them within the vacuum. Since all isotopes were enriched to more than 92% purity and thick targets were used, it was necessary to evaporate a large fraction of the expensive sample fairly uniformly on the foils. This was done by using conical tantalum evaporation boats of tapered wall thickness with current fed in radially at the opening and out at the apex to give a uniform surface temperature slightly higher than the melting point of the material. The aluminum foil was placed within a few millimeters of the top of the boat and was attached to a water-cooled heat sink. Depositions of 50–80% of the material could be obtained in this manner. The target was weighed and then scanned by observing elastic scattering of electrons from the rotating targets in order to determine the uniformity of deposition as indicated in Fig. 1. For the case of inelastic scattering, all measurements of inelastic peaks were taken relative to elastic peaks, so that a knowledge of the exact thickness was unnecessary, but it was important to keep the beam spot focused at the same radial position on the rotating target.

A typical spectrum of scattered electrons is shown in Fig. 2. The magnetic field was successively set for each experimental point shown. A typical run of an elastic peak and a strong inelastic peak would last 4 or 5 h. All points were corrected for impurities in the targets, spectrometer dispersion, counter dead-time losses, and the effects of finite resolution in angle. The widths of the peaks are due to the combined effects of beam energy spread, detector size, and ionization straggling in the target. The width of the measured elastic scattering peak for the Al target foil backing was made to equal that of the thicker Pb and Bi targets, corrected for recoil and ionization energy loss, and then subtracted from the elastic peak of the evaporated targets.

[9] V. Gillet, A. M. Green, and E. A. Sanderson, Phys. Letters **11**, 44 (1965); Nucl. Phys. **88**, 321 (1966).
[10] A. de-Shalit, Phys. Rev. **122**, 1530 (1961).
[11] G. A. Peterson and J. Alster, Phys. Rev. (to be published).
[12] G. A. Peterson, J. F. Ziegler, and R. B. Clark, Phys. Letters **17**, 320 (1965).
[13] G. A. Peterson and J. F. Ziegler, Phys. Letters **21**, 543 (1966).
[14] J. F. Ziegler and G. A. Peterson, in Proceedings of the International Conference on Nuclear Physics, Gatlinburg, Tennessee, 1966 (to be published).
[15] E. E. Bliamptis, Rev. Sci. Instr. **35**, 1521 (1964).
[16] The spectrometer was loaned to the Electron Accelerator Laboratory by the Office of Naval Research through the courtesy of Professor Robert Hofstadter of Stanford University and Dr. J. Fregeau of the Office of Naval Research.
[17] M. A. Duguay, C. K. Bockelman, T. H. Curtis, and R. A. Eisenstein, Phys. Rev. **163**, 1259 (1967).
[18] H. Crannell, R. Helm, H. Kendall, J. Oeser, and M. Yearian, Phys. Rev. **121**, 283 (1961); H. Kendall and J. Oeser, *ibid.* **130**, 245 (1963).

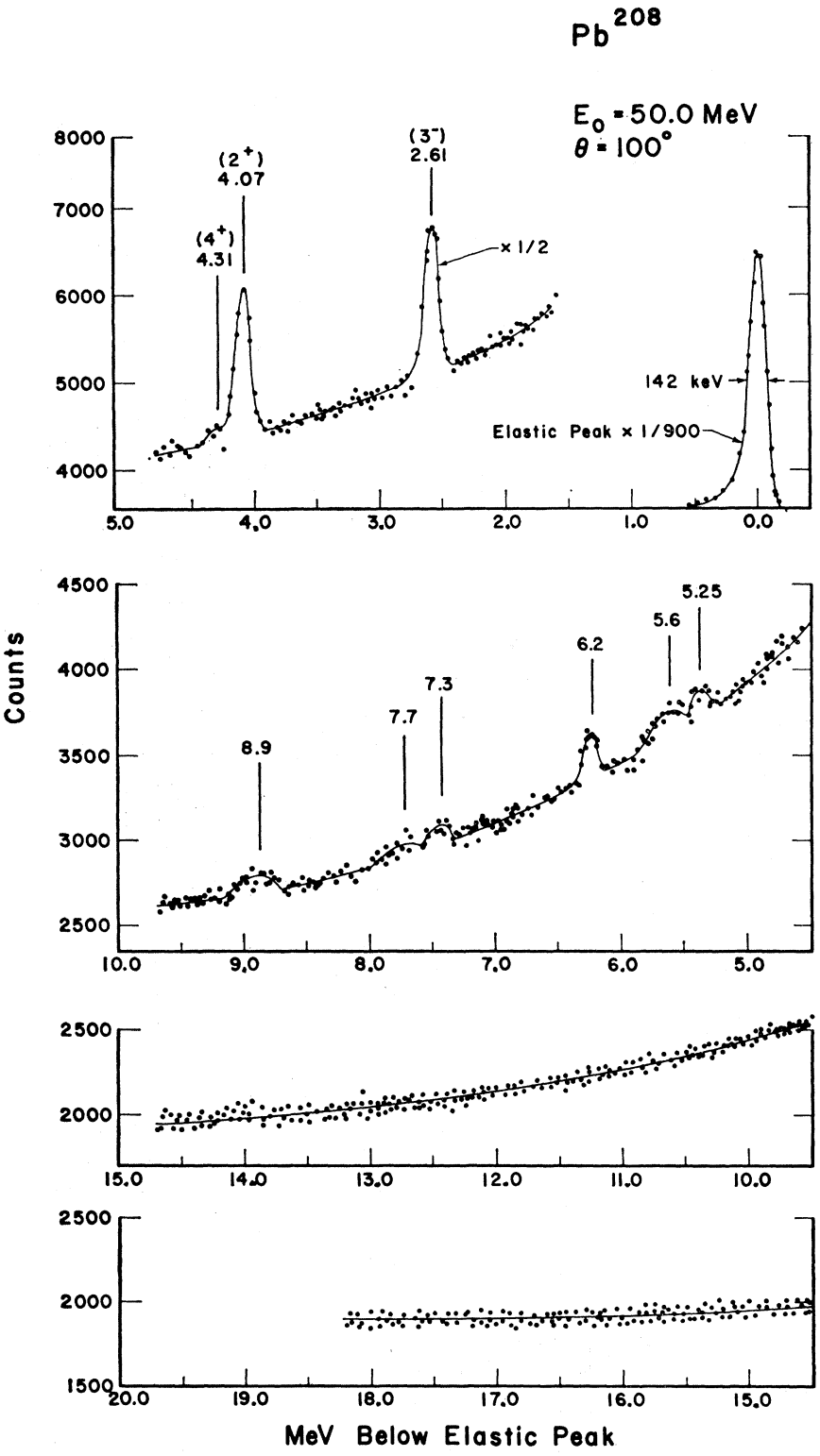

FIG. 2. The energy spectrum of electrons of initial energy 50 MeV scattered through an angle of 100° from a Pb^{208} target.

TABLE I. Values of ground-state Fermi distribution parameters as determined by electron scattering (e) and by muonic atom (μ) studies.

Method	Energy (MeV)	Target	c (10^{-13} cm)	t (10^{-13} cm)	$\langle r^2\rangle^{1/2}$ (10^{-13} cm)	Reference
μ	...	Pb^{206}	6.639±0.010	2.269±0.030	5.4894±0.0015	a
μ	...	Pb^{207}	6.629±0.012	2.317±0.034	5.4963±0.0016	a
e	53	Nat. Pb	6.66±0.09	2.21±0.17	5.48±0.07	b
μ	...	Pb^{208}	6.636±0.015	2.320±0.044	5.5026±0.0022	a
e	175	Pb^{208}	6.47±0.03	2.30±0.03	5.38±0.03	c
e	250	Pb^{208}	6.48±0.03	2.31±0.02	5.39±0.03	c
e	53	Bi^{209}	6.73±0.08	2.12±0.16	5.51±0.06	b
μ	...	Bi^{209}	6.725±0.01	2.14	5.513±0.007	d
e	150	Bi^{209}	6.69	2.24		c

[a] H. Anderson, in Proceedings of the International Conference on Electromagnetic Sizes of Nuclei, Ottawa, Canada, 1967 (to be published).
[b] G. J. C. van Niftrik and R. Engfer, Phys. Letters **22**, 490 (1966).
[c] J. Bellicard, Phys. Rev. Letters **19**, 242 (1967); (private communications).
[d] H. L. Acker, G. Backenstoss, C. Daum, J. C. Sens, and S. A. deWit, Nucl. Phys. **87**, 1 (1966).

III. ANALYSIS OF DATA

A. Cross-Section Determination

A relative inelastic cross section was obtained by multiplying the experimental inelastic-to-elastic peak area ratio C by a theoretical value of the elastic cross section σ_E in units of the Mott cross section:

$$\sigma_I(\theta,E_0)/\sigma_{\text{Mott}}=C[\sigma_E(\theta,E_0)/\sigma_{\text{Mott}}], \quad (1)$$

where

$$\sigma_{\text{Mott}}=\left(\frac{Ze^2}{2E_0}\right)^2\frac{\cos^2(\frac{1}{2}\theta)}{\sin^4(\frac{1}{2}\theta)}$$

is the cross section for the elastic scattering through an angle θ of an electron of energy E_0 from a point spinless nucleus of charge Z with no recoil. The use of such a relative cross section, $\sigma_I/\sigma_{\text{Mott}}$, eliminates most of the kinematics, makes nuclear contributions more evident, and allows a more convenient presentation of the data in analogy to that of elastic scattering. The Mott cross section is used only as a convenient unit, and its approximations do not enter into the analysis. Equation (1) implies that radiative corrections were assumed to be the same for the inelastic and elastic scattering.

In a previous measurement, the calculated elastic cross sections for Pb^{208} were experimentally checked over a large range of angles and energies.[12] Over-all agreement with the distorted-wave calculations of Fischer and Rawitscher[19] was excellent. This computer calculation agreed with those from Saclay,[20] Harvard,[21] and Darmstadt[22] to within 0.1% over the range of energies and angles of this experiment.[23] A ground-state two-parameter Fermi charge distribution[3] was assumed:

$$\rho(r)=\rho_0\left[1+\exp\left(\frac{r-c}{t/4.4}\right)\right]^{-1}, \quad (2)$$

where ρ_0 is the normalization charge density, c is the half-density radius, t is the skin-thickness measured between the 10 to 90% points of the charge distribution, and r is the nuclear radial coordinate. The values of c and t obtained by low-energy electron scattering[24] were preferred to those obtained by high-energy electron scattering, and to those obtained from precise muonic atom x-ray experiments as given in Table I. For the lead isotopes, $c=6.66$ F and $t=2.20$ F were used, and for Bi, $c=6.73$ F and $t=2.12$ F. The rms radii calculated with these values are very close to the precise muonic atom results. In this energy range the elastic scattering is mainly sensitive to the rms radius and not to small variations in c and t, whereas the high-energy results are more sensitive to the details of the charge distribution. The low-energy experiment[24] corresponds closely to this experiment; muonic atom results should be compared with electron results only for certain specific values of q.[25] Estimates of inelastic-cross-section uncertainties resulting from uncertainties in c and t are given in Sec. III D.

The inelastic peaks of Fig. 2 are situated on a continuum tail of scattered electrons resulting mainly from radiation processes in the target. For angles less than 130° this radiation tail could be calculated for small energy losses by using the Schiff peaking relation in Born approximation,[26] but with distorted-wave calculations of the elastic cross sections.[19] However, farther from the elastic peak there were uncertain contributions to the continuum due to showers caused by electrons striking the outer wall of the spectrometer vacuum chamber.[17] Therefore, instead of calculating in the usual manner[18,27] the number of expected counts Y_i in the radiation tail continuum under the peaks,

[19] C. R. Fischer and G. H. Rawitscher, Phys. Rev. **135**, B377 (1964).
[20] J. Bellicard, Phys. Rev. Letters **19**, 242 (1967); (private communication).
[21] R. Verdier (private communications).
[22] R. Engfer (private communications).
[23] J. F. Ziegler, Yale University thesis, 1967 (unpublished).
[24] G. J. C. van Niftrik and R. Engfer, Phys. Letters **22**, 490 (1966).
[25] R. Engfer, in *Proceedings of the International School of Physics "Enrico Fermi" Course, Varenna, Italy, 1966* (Academic Press Inc., New York, 1963).
[26] W. C. Barber, F. Berthold, G. Fricke, and F. E. Gudden, Phys. Rev. **120**, 2081 (1960).
[27] J. Bellicard, P. Barreau, and D. Blum, Nucl. Phys. **60**, 139 (1964).

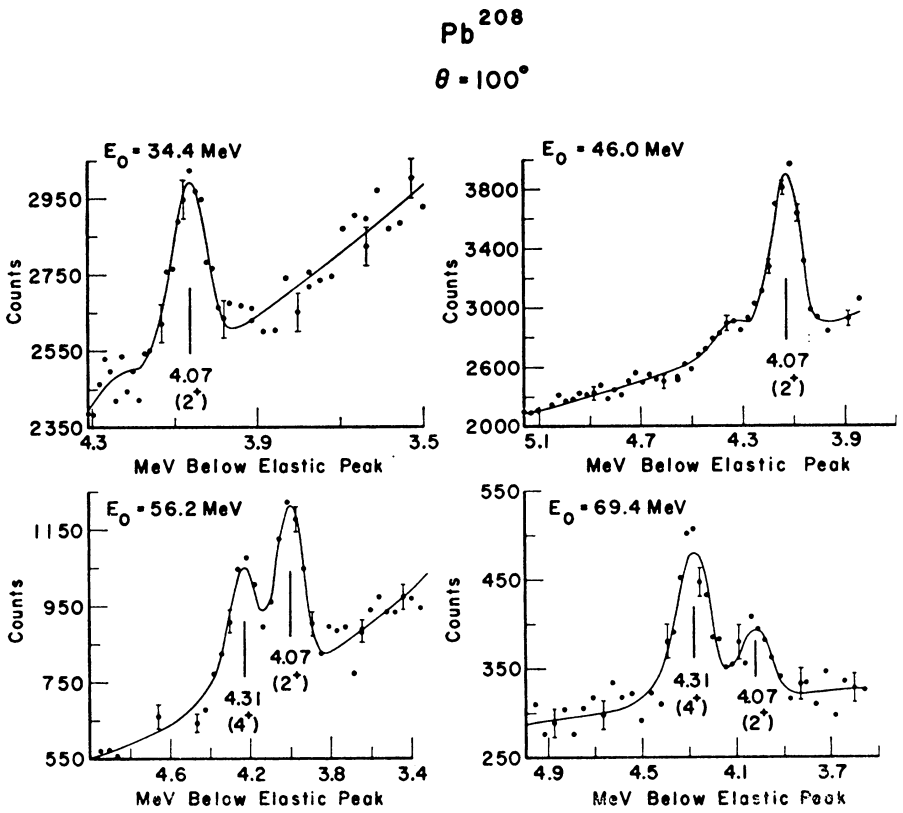

FIG. 3. Least-squares fits of the radiation tail and of the elastic peak shape to the $E2$ excitation data of Pb^{208} at 4.07 MeV and the $E4$ at 4.31 MeV for electrons scattered through an angle of 100° for four different values of initial electron energy E_0.

an empirical tail[4] and elastic peak shape of the form

$$Y_i = A(\Delta E_i)^{-1} + B(\Delta E_i)^{-2} + CP_i \qquad (3)$$

was fitted to the data where ΔE_i is the difference $E_0 - E_i$ between the energy E_0 at the elastic peak maximum and E_i at the point i on the inelastic spectrum, A, B, and C are fitting parameters, and P_i is the linearly interpolated elastic peak which was assumed to have the same shape as the inelastic peak. A χ^2 analysis gave a fitting error $\Delta C/C$ of 1 to 2% for strongly excited levels. This analysis was extended to fit two merged peaks by adding a term DP_i to Eq. (1); examples of such fits are shown in Fig. 3. The value of the coefficient C (or D), corresponding to the best χ^2 fit, is the ratio of the inelastic to elastic peak area. Excitation energies of strong excited peaks were determined to about ±40 keV.

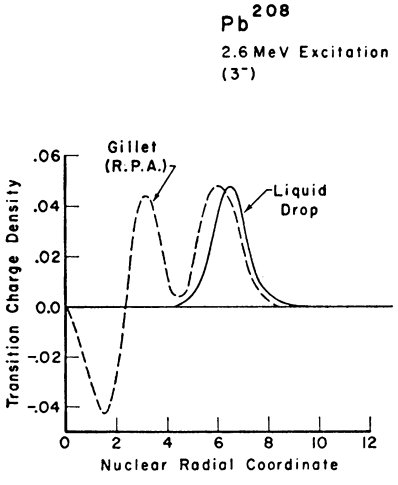

FIG. 4. Transition charge density as a function of nuclear radial coordinate for the 2.614-MeV (3⁻) excitation in Pb^{208} calculated according to the Gillet random-phase-approximation assumption and according to the Tassie hydrodynamical model with arbitrary normalization of the latter.

B. Born-Approximation Calculations

It is instructive to consider plane-wave Born-approximation calculations before considering parameter extraction by use of distorted-wave formalism.

Including only the Coulomb or longitudinal contributions in Born approximation, the relative cross section for an electric multipole (EL) excitation of a spinless nucleus is,[1]

$$\frac{\sigma_I(\theta,E_0)}{\sigma_{\text{Mott}}} = \frac{4\pi}{Z^2}[2L+1]\left[\int j_L(qr)Y_{LM}(\Omega)\rho_{fi}(\mathbf{r})d\tau^3\right]^2, \qquad (4)$$

where $j_L(qr)$ is a spherical Bessel function of order L, $Y_{LM}(\Omega)$ is a spherical harmonic, and $\rho_{fi}(\mathbf{r})$ is the reduced nuclear-transition charge density between the initial and final nuclear states i and f for a nuclear charge operator $\hat{\rho}$:

$$\rho_{fi}(\mathbf{r}) = \langle f\|\hat{\rho}\|i\rangle .$$

The three-momentum transfer q must take into account[5] the excitation energy ϵ of the nucleus of mass M:

$$q=\frac{2E_0}{\hbar c}\frac{\sin\frac{1}{2}\theta}{(1+(2E_0/Mc^2)\sin^2\frac{1}{2}\theta)^{1/2}}\times\left\{1-\frac{\epsilon}{E_0}+\frac{1}{1+(2E_0/Mc^2)\sin^2\frac{1}{2}\theta}\times\left[\frac{\epsilon}{Mc^2}+\left(\frac{E_0}{Mc^2}\right)^2\sin^2\tfrac{1}{2}\theta+\left(\frac{\epsilon}{2E_0}\right)^2\frac{1}{\sin^2\frac{1}{2}\theta}\right]\right\}^{1/2}.$$

For this experiment, this may be approximated within 1% by

$$q\approx\frac{2E_0\sin\frac{1}{2}\theta}{\hbar c}\left(1-\frac{\epsilon}{E_0}\right)^{1/2}.$$

The use of a common reduced-transition charge density of the form

$$\rho_{fi}(\mathbf{r})=\rho_{\rm tr}(r)Y_{LM}^*(\Omega)$$

results in a relative cross section

$$\frac{\sigma_I(\theta,E_0)}{\sigma_{\rm Mott}}=\frac{4\pi}{Z^2}[2L+1]\left[\int j_L(qr)\rho_{\rm tr}(r)r^2dr\right]^2. \quad (5)$$

An examination of this equation shows the Born-approximation cross-section dependence upon momentum transfer q. Figure 4 shows two markedly different arbitrarily normalized transition charge densities for the 2.6-MeV electric octupole excitation of Pb^{208}. One is the transition charge density for the incompressible and irrotational vibrating-liquid-drop model of Tassie,[8]

$$\rho_{\rm tr}=N_L r^{L-1}\partial\rho/\partial r, \quad (6)$$

where ρ is the ground-state charge density of Eq. (2), N_L is a normalizing factor depending on Z, surface

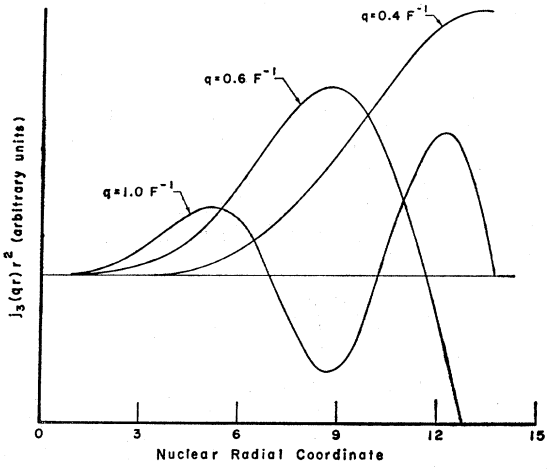

FIG. 5. The third-order spherical Bessel functions weighted by the square of the nuclear radial coordinate versus the nuclear radial coordinate with momentum transferred to the nucleus as a parameter.

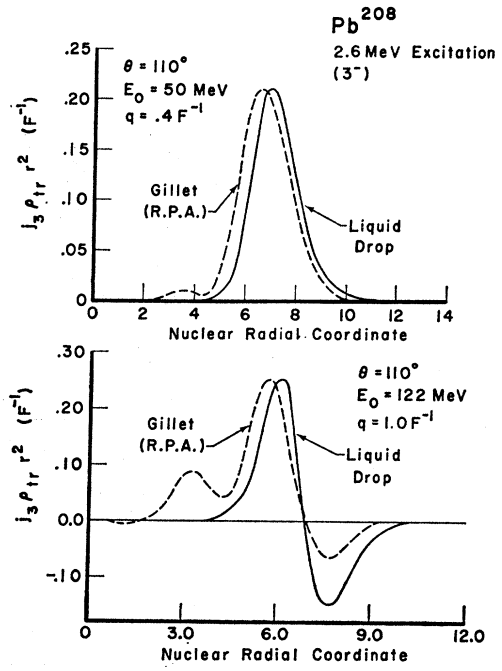

FIG. 6. The integrand of Eq. (5) versus the nuclear radial coordinate for the 2.6-MeV excitation of Pb^{208} evaluated at a scattering angle of 110° and incident electron energies of 50 and 122 MeV for the Tassie liquid-drop model and for the Gillet random-phase-approximation model.

tension, etc. The other is the Gillet random-phase-approximation (RPA) result for the 2.6-MeV, $L=3$ transition in Pb^{208}. This shell-model calculation takes into account nucleon correlations in both the excited and the ground states.[9,28] Figure 5 shows the third-order spherical Bessel function weighted by r^2, and Fig. 6 shows the two transition charge densities multiplied by $r^2j_3(qr)$, the integrand of Eq. (5), for two different momentum transfers q. This illustrates that the integrands and hence the Born-approximation cross sections of Eq. (5) are quite different for the higher q, but are similar for the lower q. For the higher q the inner structure of the transition charge density enters significantly, whereas for the lower q only the surface details of the transition charge density affect the cross section. Because of the shell structure in the Gillet $\rho_{\rm tr}$, its integrand reduces mostly to a single peak at the nuclear surface for low-q calculations.

The use of the Wigner-Eckart theorem and the expansion of $j_L(qr)$ in Eq. (4) gives[29]

$$\frac{\sigma_I}{\rho_{\rm Mott}}=\frac{q^{2L}4\pi B(EL)}{Z^2[(2L+1)!!]^2}\left[1-\frac{q^2}{2(2L+3)}R_{\rm tr}^2+\cdots\right], \quad (7)$$

where the reduced nuclear transition probability

$$B(EL,0\rightarrow L)=(2L+1)\left(\int r^LY_{LM}\rho_{fi}(\mathbf{r})d\tau^3\right)^2, \quad (8)$$

[28] V. Gillet, private communications to J. F. Ziegler.
[29] R. S. Willey, Nucl. Phys. **40**, 529 (1963).

and the transition radius R_{tr} is defined by

$$R_{tr}^2=\frac{\int r^{L+2}Y_{LM}\rho_{fi}(\mathbf{r})dr^3}{\int r^L Y_{LM}\rho_{fi}(\mathbf{r})dr^3}. \quad (9)$$

Thus in Born approximation $B(EL)$ and R_{tr} may be obtained by fitting Eq. (6) to low-q experimental cross sections. The extrapolation of $(\sigma_I/\sigma_{\text{Mott}})q^{-2L}$ to $q=0$ is proportional to $B(EL)$; the initial rate at which this quantity falls off as q^2 increases is proportional to R_{tr}^2.

An estimation was made of the contribution to the cross section by the next term of the expansion in Eq. (7) by using a δ-function transition charge density at the nuclear surface. For an electric quadrupole excitation of Pb^{208} at $q=0.4$ F^{-1}, this term is about 0.1 of the second term and hence would give an insignificant contribution. This indicates that $B(EL)$ and R_{tr} sufficiently describe ρ_{tr} for Born-approximation cross sections in a range of low q.

C. Distorted-Wave Calculations and Model Dependence

The use of a distorted-wave calculation, such as GBROW,[6,7] is mandatory for the inelastic scattering conditions of this experiment. This is evident in Fig. 7 which shows that the use of the plane-wave Born approximation would give incorrect values of the inelastic cross sections calculated using Tassie's model.[8] Also there would be uncertainties in the assignment of multipolarities by use of the Born approximation, as can be seen by noting the positions of the maxima and minima for the plane-wave and distorted-wave cases. Note that although the cross section of Fig. 7 is conveniently plotted versus q, in the distorted-wave case cross sections are not functions of q alone as in the Born approximation, but are functions separately of θ and E_0.

The GBROW calculations[6,7] take into account the effects of finite excitation energy and include both transverse electric and longitudinal electric contributions. In the Tassie model[8] the transverse contributions are small below 150°. For example, they are largest at the diffraction minima of the curve for the electric quadrupole excitation of Pb^{208} as shown in Fig. 7, where they amount to 2% of the total.

Five conditions are assumed in the GBROW code: (1) The transition is of an electric multipole character, (2) the ground state is spherically symmetrical, (3) nuclear recoil energy is negligible compared to the excitation energy, (4) the interaction involved is free of polarization or dispersion effects, and (5) the excited-state charge distribution is not significantly distorted from that of the ground state.

That the first condition is fulfilled may be verified for the observed levels experimentally. If magnetic contributions are present, they will systematically enhance the cross sections at back angles.[1] It will be shown that such contributions are not discernible in the levels considered.

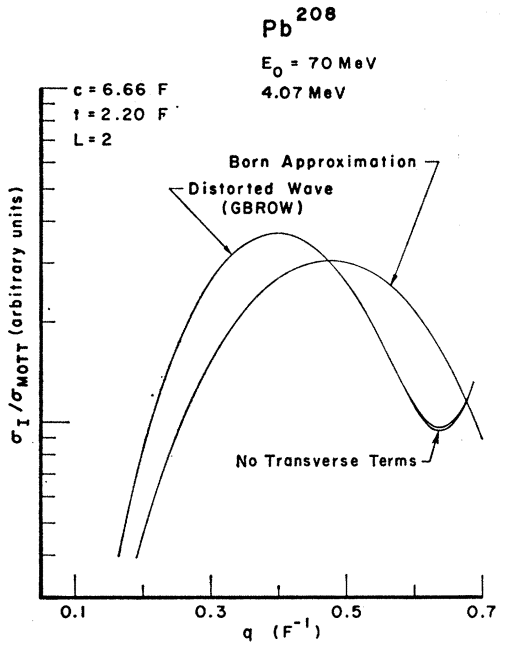

FIG. 7. Relative cross sections versus momentum transferred to the nucleus for an electric quadrupole excitation of Pb^{208} at 4.07 MeV calculated according to the plane-wave Born approximation and the distorted-wave GBROW code assuming the Tassie hydrodynamical model. The GBROW code includes transverse electric contributions which are largest (about 2% of the total) at the diffraction minimum.

Condition 2 is satisfied because the doubly closed shell (or nearly so) heavy nuclei of this experiment are expected to be nearly spherical.

Condition 3 is satisfied because the largest nuclear recoil is 50 keV in this experiment and this is far less than the lowest observed excitation energy of about 2.6 MeV.

Condition 4 concerns dispersion effects of virtual excitations and de-excitations. These have been too small to be observed in the ground state[12] and should also be small for excited states.[30] This is treated further in Sec. IV.

With regard to condition 5, one indication of distortion of the excited state is to consider the number of particles taking part in the transition. Gillet[28] estimates by a shell-model RPA calculation for Pb^{208} a single-particle reduced-transition probability $B(E3)$ of $0.11e^2b^3$, compared to $0.018e^2b^3$ obtained from the familiar Weisskopf single-particle relation[31]:

$$B(EL, 0\rightarrow L)_{sp} = e^2[(2L+1)/(4\pi)][3R_0^L/(3+L)]^2, \quad (10)$$

where $R_0=1.20A^{1/3}$ F.

[30] G. H. Rawitscher, Phys. Rev. **151**, 846 (1966).
[31] J. M. Blatt and V. W. Weisskopf, *Theoretical Nuclear Physics* (John Wiley & Sons, Inc., New York, 1952), p. 627.

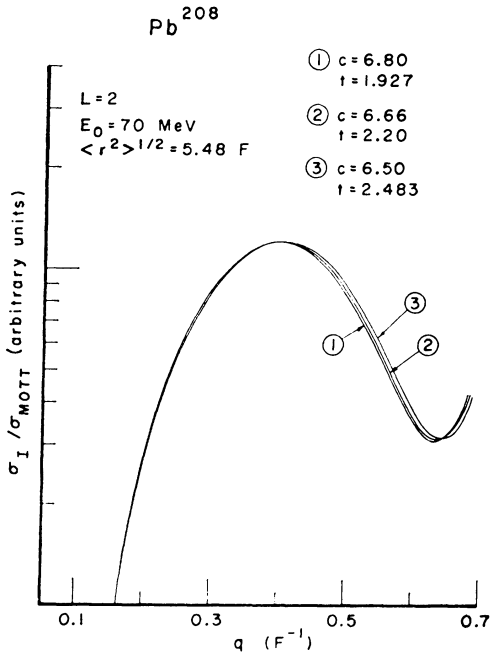

FIG. 8. Relative cross sections versus momentum transferred to the nucleus for an electric quadrupole excitation of Pb^{208} at 4.07 MeV calculated according to the GBROW distorted-wave code for different sets of Fermi-model ground-state parameters. All sets yield an rms ground-state radius of 5.48 F.

Using the RPA method, it is found that only seven particles or 3% of the total number of particles take part in the $E3$ excitation at 2.615 MeV of Pb^{208}. This should not give rise to a significant distortion of the excited state from that of the ground state.

The GBROW distorted-wave calculations are normalized by dividing by[32]

$$K=(2L+1)\left[\frac{(2L+1)!!}{q^L}\int j_L(qr)\rho_{tr}(r)r^2dr\right]^2. \quad (11)$$

This normalizes the GBROW transition matrix elements to a unit transition probability, $B(EL)=1.0e^2b^L$ (where $b=10^{-24}$ cm^2), as in the Alder, Bohr, Huus, Mottelson, and Winther formalism.[6,7] One advantage of this normalization is the elimination of any non-radial-dependent coefficients of ρ_{tr}, such as the surface-tension parameter in the liquid-drop model, and the effects of nonzero ground-state spins.

In order to estimate model dependence of the calculation, it is necessary to estimate the effects of the nuclear ground state and the transition-charge-density models on the $B(EL)$'s.

Ground-state model dependency was tested by showing that GBROW calculations of cross sections are sensitive mainly to the rms radius of the ground state and not to a more detailed model such as the two-parameter Fermi model of Eq. (2). Figure 8 shows the effect on the relative cross section of varying the Fermi-model ground-state parameters c and t over large ranges for an electric quadrupole transition in Pb^{208}. The rms radius of 5.48 F and the transition charge density were held constant. Only the ground-state charge density was changed. Parameter sets 1 and 3 represent the limits on c and t from the best experimental determination of Engfer and van Niftrik.[24] The difference, as shown in Fig. 8, resulting from using parameter sets 1 and 3, from the accepted set 2, is less than 0.8% at the maximum of the curve, and 1.9% beyond it for the range of q shown. A similar computation made for an electric octupole transition in Pb^{208} shows that changes in cross section are smaller by a factor of about 2 for this higher multipolarity for the same variation of c and t.

In Born-approximation calculations we have indicated that $B(EL)$ and R_{tr}, the Lth and "$L+2$" moment of ρ_{tr}, sufficiently describe ρ_{tr} for the low q of this experiment. As was shown in Sec. III B, Gillet's complex ρ_{tr} reduced approximately to a single peak at the nuclear surface when weighted by the kinematic terms for low q in the integrand of Eq. (5). This reduction to a single peak is anticipated here whenever ρ_{tr} shows definite shell structure.

To test the hypothesis that $B(EL)$ and R_{tr}, in distorted-wave calculations, still are sufficient to describe ρ_{tr}, we have made trial calculations using a wide range of single peaks at the nuclear surface, which have a constant $B(EL)$ and R_{tr}.

Test variations in ρ_{tr} were calculated by decoupling c and t of Eq. (6) from the ground state, and arbitrarily defining them to obtain the desired $B(EL)$ and R_{tr}. For example, Fig. 9 shows two ρ_{tr}'s with the same $B(EL)$ and R_{tr} of a quadrupole vibrating-liquid-drop excitation in Pb^{208}. The results of sample calculations are shown in Fig. 10 for both quadrupole and octupole

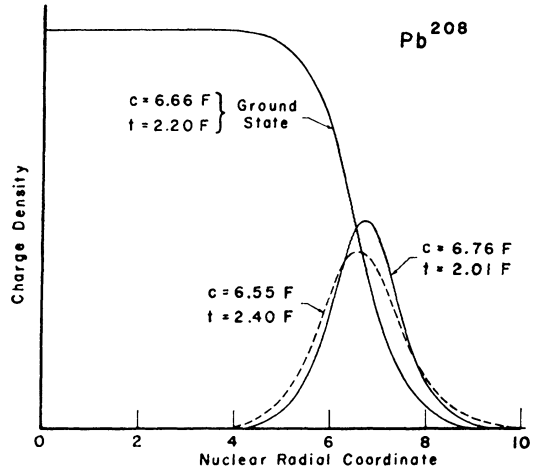

FIG. 9. The radial dependence of the Pb^{208} ground-state charge density and two transition charge densities calculated for different values of the ground-state parameters for an electric quadrupole excitation of Pb^{208} normalized to 30 single-particle units.

[32] Reference 7, pp. 94–107.

excitations. The ground-state charge density was held constant. The values of c and t shown were used to calculate test ρ_{tr}'s using Eq. (6), where ρ refers to a Fermi shape. These yielded the plotted cross sections. The vibrating-liquid-drop model has cross-section curves which fall about midway between each pair.

Again as in Fig. 8, the differences in the relative inelastic cross sections from the liquid-drop model are very small: less than 1.2% over the range of q of this experiment and less than 0.3% at the maximum of the relative inelastic cross sections. The latter difference is of the order of the expected accuracy of the numerical calculations.[7]

The above arguments indicate that our expected nuclear-model dependence may be assumed to be about $\pm 2\%$.

IV. EXPERIMENTAL RESULTS AND DISCUSSION

A. Nuclear Parameter Extraction

In order to obtain results over a broad range of q, data were taken at various angles and energies depending upon accelerator operating conditions. A table of the experimentally determined cross sections is available on request.[23]

To determine the multipolarity of a transition, for a case where the statistics are poor, the best practical way is to note where the relative cross-section peaks as a function of q. The multipolarity can not be determined for large L and Z by noting a slope proportional to q^{2L}, as has been suggested.[6]

To extract $B(EL)$, the experimental values of $\sigma_I/\sigma_{\text{Mott}}$ were compared to the calculated values from

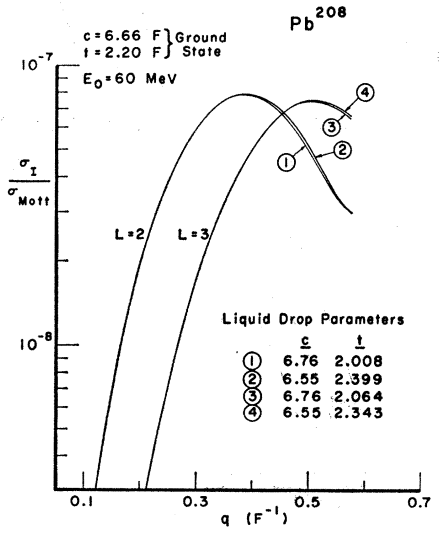

FIG. 10. Relative cross sections versus momentum transferred to the nucleus for an $E2$ excitation at 4.07 MeV and an $E3$ excitation at 2.61 MeV for Pb^{208} calculated according to the GBROW distorted-wave code for different sets of transition charge density parameters. The transition radius was held constant at 7.28 F for the $E2$ excitation, and a 7.30 F for the $E3$ excitation.

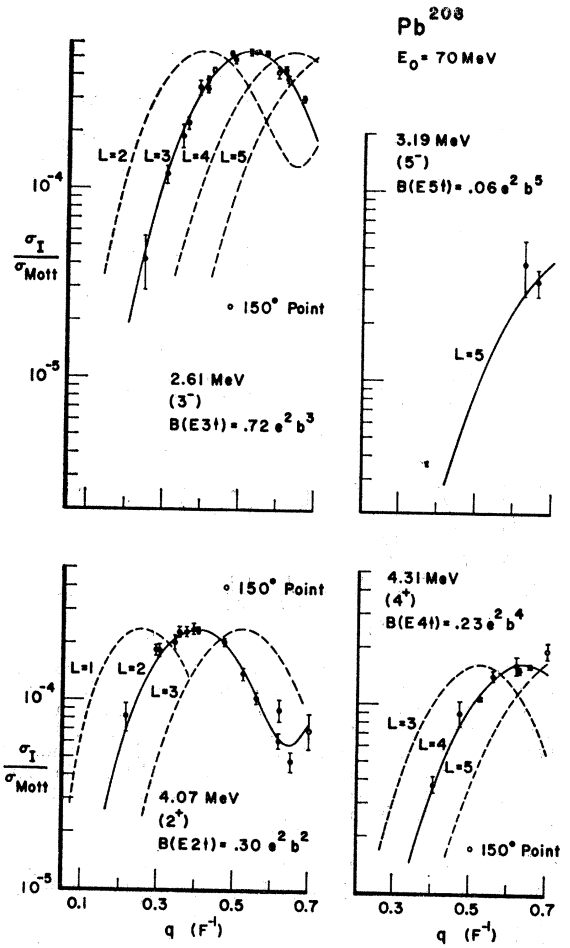

FIG. 11. Experimental relative cross sections versus momentum transferred to the nucleus Pb^{208} normalized to an initial electron energy of 70 MeV for excitations at 2.61, 3.19, 4.07, and 4.31 MeV. The solid curve is the best fit of the GBROW calculation assuming the Tassie hydrodynamical model for the specified transition multipolarity, and the dashed curves are arbitrarily normalized for other transition multipolarities.

GBROW for each energy and angle. The ratio will give directly the $B(EL)$ as determined by that datum. Note that these $B(EL)$'s are defined by the normalization of Eq. (11). These values of $B(EL)$ were based upon the use of the ground-state parameters of Engfer and van Niftrik[24] for both the elastic and inelastic scattering. If the ground-state parameters of Bellicard,[20] determined by high-energy electron scattering, were used, values of $B(EL)$ generally a few percent lower would result.[23]

It is very difficult to display the results directly, for there will be a separate GBROW curve for each incident energy. For purposes of evaluating the scatter of data, therefore, all data points were normalized to the same energy (70 MeV). This normalization is done by comparing the data point to the specific calculation of GBROW for that angle and energy, then keeping the value of q_I (inelastic momentum transfer) constant,

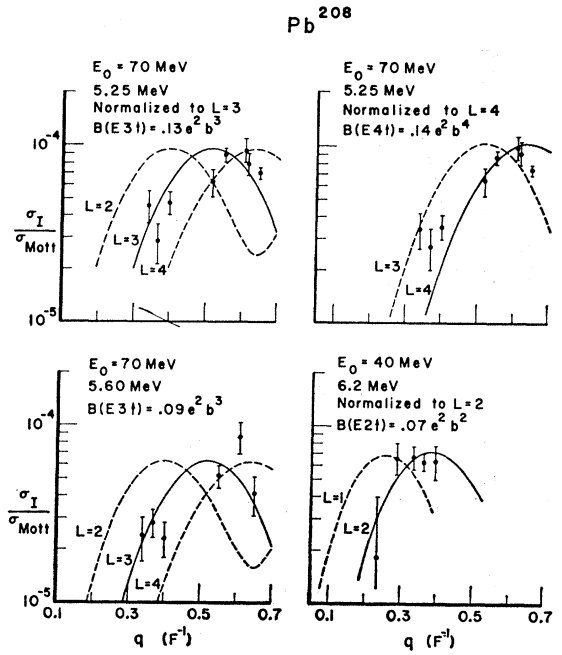

FIG. 12. Experimental relative cross sections versus momentum transferred to the nucleus Pb^{208} normalized to an initial electron energy of 70 MeV for excitations at 5.25 and 5.60 MeV, and to an initial energy of 40 MeV for the 5.2-MeV excitation. The solid curve is the best fit of the GBROW calculation assuming the Tassie hydrodynamical model for the specified transition multipolarity, and the dotted curves are arbitrarily normalized for other transition multipolarities.

displacing it from the 70-MeV GBROW curve by the same percentage as it was from its explicit GBROW point.

This normalization to 70 MeV shows directly *the scatter of data* about the theoretical calculation.

The experimental relative cross sections are presented in Figs. 11 through 15 compared to the GBROW Tassie vibrating-liquid-drop calculations whose transition multipolarity seems best to agree with the data points. Since the various GBROW curves differ markedly with multipolarity, there is only one very weak level for which more than one normalization is necessary: The 5.25 MeV level in Pb^{208} is shown normalized both to $L=3$ and $L=4$ curves.

The validity of the vibrating incompressible irrotational liquid-drop nuclear model was tested extensively on the three large collective states in Pb^{208}: 2.614 MeV (3^-), 4.07 MeV (2^+), and 4.31 MeV (4^+) as shown in Fig. 11.

The best test was for the 3^- level, as its very large strength allowed it to be tested accurately over a wide range of q. As the plot shows, the fit is excellent. The 2^+ level was similarly tested over a wide range of momentum transfer, but its strength was much lower and so the errors associated with its measurement were greater. This fit is good, except at low q, where the data points are rather high. The three lowest q points, if they are truly high, seem to indicate that the transition charge density of the liquid drop does not have enough amplitude on its outer tail. This, in the Born approximation, is the part of ρ_{tr} which is dominant for low q, and which becomes less significant for higher q when the Bessel function peak amplifies more of the inner structure of the transition charge density (see Fig. 6).

The 4^+ level rises only at high q and could be measured over only a limited range, but the use of the Tassie model gave a good fit to the data.

We conclude that the incompressible irrotational vibrating liquid drop is satisfactory for fitting these levels, within the 2% model dependence of the calculations.

If there were magnetic or transverse electric contributions arising from nuclear currents, an enhancement of the cross sections at backward angles would be expected.[1] No enhancement was observed at 150° scattering angle, as is indicated by the open circle points of Figs. 11 through 15. The small amount of transverse electric contribution in the Tassie model for the Pb^{208} $E2$ excitation is indicated in the caption to Fig. 7.

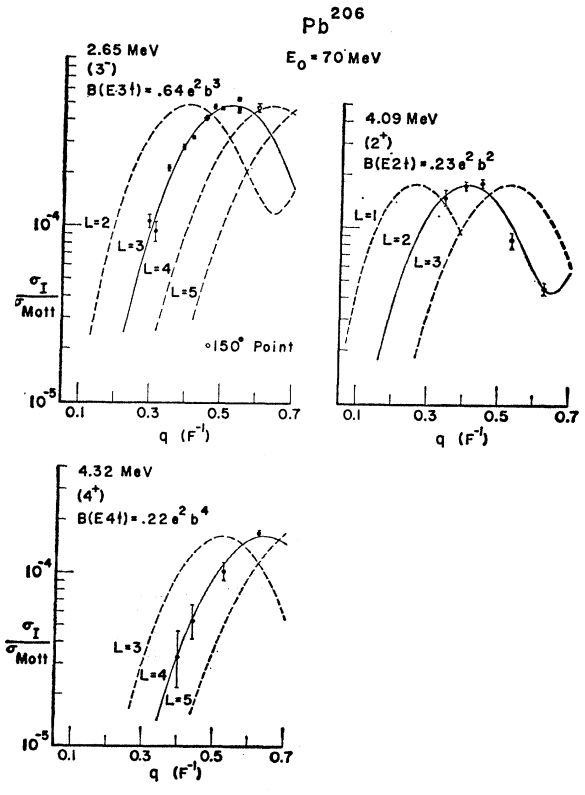

FIG. 13. Experimental relative cross sections versus momentum transferred to the nucleus Pb^{206} normalized to an initial electron energy of 70 MeV for excitations at 2.649, 4.09, and 4.32 MeV. The solid curve is the best fit of the GBROW calculation assuming the Tassie hydrodynamical model for the specified transition multipolarity and the dashed curves are arbitrarily normalized for other transition multipolarities.

The values of the extracted reduced nuclear transition probabilities are given in Table II together with those of other experiments. The errors given include the 2% for model dependence, as discussed in Sec. III C.

Since good agreement with Tassie's liquid-drop model was obtained, as indicated in Figs. 11 through 15, the values of R_{tr} were calculated for the lead isotopes by use of Eq. (9). With $c=6.66$ F and $t=2.20$ F, $R_{tr}=7.3$, 7.5, and 7.7 F for $L=2$, 3, and 4, respectively. For Bi^{209}, with $c=6.73$ F and $t=2.12$ F, $R_{tr}=7.5$ F for $L=3$.

The role and importance of the transition radius R_{tr} in understanding nuclear structure remains to be clarified. It may provide information about nuclear surfaces and serve as an important number for the testing of nuclear wave functions as does $B(EL)$. Values of R_{tr} reported thus far are larger than the half-density radius of the ground state and seem to increase as the multipolarity increases. Values of $R_{tr}A^{-1/3}$ are relatively constant with A for the same multipolarity and are larger for longitudinal electric than for transverse magnetic excitations.[5,17]

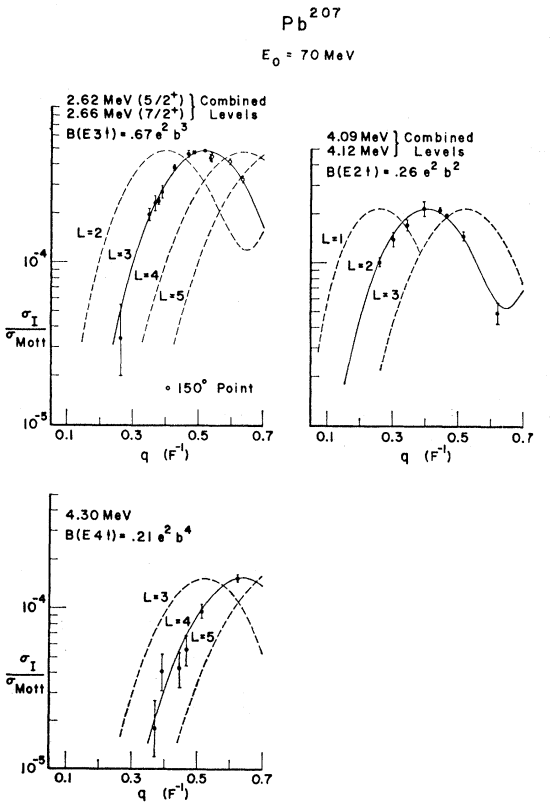

FIG. 14. Experimental relative cross sections versus momentum transferred to the nucleus Pb^{207} normalized to an initial electron energy of 70 MeV for excitations at about 2.6, 4.1, and 4.39 MeV. The solid curve is the best fit of the GBROW calculation assuming the Tassie hydrodynamical model for the specified transition multipolarity, and the dashed curves are arbitrarily normalized for other transition multipolarities.

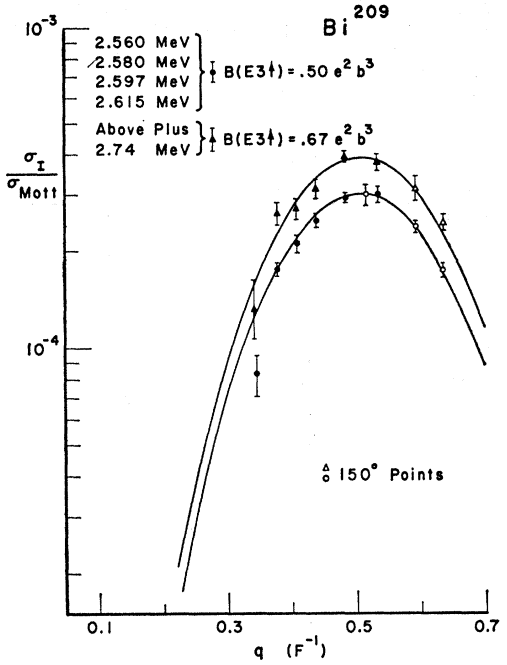

FIG. 15. Experimental relative cross section versus momentum transferred to the nucleus Bi^{209} normalized to an initial electron energy of 70 MeV for the group of excitations at about 2.6 MeV. The solid curves are the best fits of the GBROW calculation assuming the Tassie hydrodynamical model for an $L=3$ transition.

B. Discussion of Excitations

There are many levels known other than those excited in this experiment.[33–36] At the scattering angles of 150° and forward, magnetic excitations would tend to be suppressed relative to electric excitations,[1,29] and would not be observed. Furthermore single-particle and weak transitions would be less evident for these high-Z isotopes compared to collective electric excitations, which could be observed above the large radiation tails. For example, note the large radiation tail and the suppression of the ordinate scale in Fig. 2. In regions near the elastic peak where the radiation tail is exceptionally large, even collective excitations, such as the first excited state in Pb^{206} at 0.803 MeV, could not be observed above the radiation tail. Also the accelerator used in this experiment[23] is capable only of giving $q \gtrsim 0.75$ F^{-1}, so that for these heavy nuclei, multipolarities of 5 and greater, such as seen by (p,p') at Saclay,[34] would be difficult to observe.

Figure 3 shows Pb^{208} data in the region of 4-MeV excitation for a scattering angle of 100° and various

[33] A comprehensive review of the nuclei in the lead region has recently been given by E. K. Hyde, I. Perlman, and G. T. Seaborg, *The Nuclear Properties of the Heavy Elements* (Prentice-Hall, Inc., Englewood Cliffs, N. J., 1964).

[34] J. Sandinos, G. Vallois, O. Beer, M. Gendrot, and P. Lopato, Phys. Letters **22**, 492 (1966).

[35] G. Vallois, J. Sandinos, O. Beer, M. Gendrot, and P. Lopato, Phys. Letters **22**, 659 (1966).

[36] G. Vallois, J. Sandinos, and O. Beer, Phys. Letters **24B**, 512 (1967).

TABLE II. Experimental values of reduced nuclear transition probabilities $B(EL)$ for the excitation of a nucleus from its ground state to an excited state as determined by the electron scattering methods of this experiment and by other methods. The units of $B(EL)$ are e^2b^L where e is the electron charge, b is 10^{-24} cm^2 (1 b), and L is the multipolarity of the transition. $B(EL)_{sp}$ is the single-particle estimate of Eq. (10).

			This experiment			Other experiments
Nuclide	Level (MeV)	Transition character	$B(EL, 0\rightarrow L)$ e^2b^L	$G=\frac{B(EL)}{B(EL)_{sp}}$	Ref.	$B(EL, 0\rightarrow L)$ e^2b^L
Pb^{206}	4.09	$E2$	0.23±0.02	6.2	a	(p,p')0.20
Pb^{207}	4.090[b] 4.125[b]	$E2$	0.26±0.02	7.0	c d	(α,α')0.33 (p,p')0.18
Pb^{208}	4.07	$E2$	0.30±0.02	8.1	c e	(α,α')0.33 (p,p')0.17
Pb^{206}	2.65	$E3$	0.64±0.04	35	a	(p,p')0.33
Pb^{207}	2.625[b] 2.664[b]	$E3$	0.67±0.04	37	c d	(α,α')0.56 (p,p')0.32
Pb^{208}	2.614	$E3$	0.72±0.04	39.5	c f g e h i j k	(α,α')0.57 (e,e')0.53 (p,p')0.67 (p,p')0.36 $(C^{12},C^{12}\gamma)$0.83 (p,p')0.84 (p,p')0.97 (n,n')0.71
Bi^{209}	2.6[l]	$E3$	0.67±0.05	37	c f m	(α,α')0.57 (e,e')0.55 (p,p')0.65
Pb^{206}	4.32	$E4$	0.22±0.02	25	a	(p,p')0.058
Pb^{207}	4.29	$E4$	0.21±0.03	24	c	(α,α')0.12
Pb^{208}	4.31	$E4$	0.23±0.02	26	c f e	(α,α')0.13 (e,e')0.24 (p,p')0.057
Pb^{208}	5.25	$E3$ $(E4)$	0.13±0.03 0.14±0.07	7.2 16		
Pb^{208}	5.6	$E3$	0.09±0.03	5	c	(α,α')0.16
Pb^{208}	6.2	$E2$ $(E0)$	0.07±0.02	2		
Pb^{208}	3.2	$E5$	0.06±0.02	14	c e	(α,α')0.03 (p,p')0.034

[a] G. Vallois, J. Sandinos, and O. Beer, Phys. Letters **24**, 512 (1967).
[b] Peaks were not resolved in this experiment. Energies taken from J. C. Hafele and R. Woods, Phys. Letters **24**, 579 (1966).
[c] J. Alster, Phys. Rev. **141**, 1138 (1966); Phys. Letters **25B** 459 (1967).
[d] G. Vallois, J. Sandinos, O. Beer, M. Gendrot, and P. Lopato, Phys. Letters **22**, 659 (1966).
[e] J. Sandinos, G. Vallois, O. Beer, M. Gerdrot, and P. Lopato, Phys. Letters **22**, 492 (1966).
[f] H. Crannell, R. Helm, H. Kendall, J. Oeser, and M. Yearian, Phys. Rev. **123**, 923 (1961); and H. W. Kendall and J. Oeser, *ibid.* **130**, 245 (1963).
[g] A. Scott and M. P. Fricke, Phys. Letters **20**, 654 (1966).
[h] A. Z. Hrynkiewicz, S. Kopta, S. Szymczyk, and T. Walczak, Nucl. Phys. **79**, 495 (1966), references cited therein, and see text of this section.
[i] G. R. Satchler, R. H. Bassel, and R. M. Drisko, Phys. Letters **5**, 256 (1963).
[j] T. Stovall and N. M. Hintz, Phys. Rev. **135**, B330 (1964).
[k] P. H. Stelson *et al.*, Nucl. Phys. **68**, 97 (1965).
[l] Approximate energy of seven unresolved peaks, J. C. Hafele and R. Woods, Phys. Letters **24**, 579 (1966).
[m] S. Hinds, H. Marchant, J. H. Bjerregaard, and O. Nathan, Phys. Letters **20**, 674 (1966).

incident energies. This illustrates qualitatively the q dependence of the inelastic cross sections for different multipolarities.

Pb^{208} Levels

The strongest excitations seen in all isotopes in this experiment were the well-known octupole excitations[37] at about 2.6 MeV as given in Table II. This state in Pb^{208} is the highest first excited state in any nucleus with A greater than 40, an indication of closed-shell stability. Our results are in the middle of the scatter of previously reported results. As Fig. 11 shows, the fits to the theoretical curves calculated under the assumption of the Tassie hydrodynamical model[8] are excellent. It should be noted that the Tassie model leaves *no free parameters* in the extraction of $B(EL)$. This experiment, which shows no disagreement with the macroscopic Tassie model, points out the need for higher-momentum-transfer experiments to show more details of the transition charge density.

Other models have been used to attempt to explain this octupole excitation. Lane and Pendlebury[37] have considered vibrational configurations involving phonons of an octupole surface deformation.

Gillet, Green, and Sanderson[9] have calculated excitation energies and transition probabilities in

[37] A. M. Lane and E. D. Pendlebury, Nucl. Phys. **15**, 39 (1960).

Pb^{208} by using a one-particle–one-hole calculation in the context of the random phase approximation involving nucleon correlations in both the excited and ground state. Their transition charge densities differ markedly from the usual vibrational model as shown in Fig. 6. The inelastic scattering of electrons has been calculated using GBROW for the RPA ρ_{tr}.[38] Although the RPA increases noticeably the absolute values of the cross section as compared with the results of the ordinary particle-hole model, the RPA cross sections were smaller than experimental values by a factor of 3 for the 3^-, 2.6-MeV state in Pb^{208}, and by a factor of 2 for the 5^-, 3.15-MeV state.

Le Tourneux and Eisenberg[39] have applied a zero-range surface delta interaction (SDI), together with particle-hole formalism to closed-shell nuclei and have treated Pb^{208} in detail in both the Tamm-Dancoff (TD) approximation (where only excited-state correlations are taken into account) and in the random phase approximation. The SDI-RPA work agrees closely with that of Gillet.

Other highly collective transitions seen in our studies[13] were the $E2$ and $E4$ at about 4.1 and 4.3 MeV in all isotopes. The $E2$ transition probably was first seen in natural Pb by Barber *et al.*[26] by the scattering of 40-MeV electrons. Later Crannell *et al.*[18] reported an excitation in Pb^{208} at 4.3 MeV in a high-q but coarse resolution experiment, which was given a 4^+ assignment. That experiment did not give a convincing fit to the distorted-wave calculations,[6] most likely because the 2^+ and 4^+ states were unresolved. Alster[40] in an (α,α') experiment resolved the two states in Pb^{208} but was unable to make definite assignments of spin and parity: 2^+ was preferred for both states, but 4^+ was possible. Scott and Fricke[41] in a (p,p') experiment, identified these states as 2^+ and 5^-. According to Fig. 11, the 4.07-MeV state is 2^+ and the 4.31-MeV state is 4^+. It should be noted[42] that $E0$ and $E2$ excitations have similar q dependences in certain models. However, Alster's[40] results exclude an assignment of 0^+ to the 4.07-MeV state because no inhibition of the excitation was shown in his study, and (α,α') scattering does not strongly excite monopole states.

Recent tentative reports[34,41,43] indicate that near the 4.3-MeV 4^+ level in Pb^{208} there may either a 5^- or 6^+ level, or both. If this is true, this would explain the high datum point at $q=0.7$ F^{-1} where these levels would just begin to contribute to the 4^+ peak analyzed.

The 5.25-MeV level of Pb^{208} has not been reported before. Bellicard has seen a level at 5.30 MeV with 150-MeV electron scattering, and has tentatively suggested[20] a 4^+ assignment. Our work indicates an assignment of either 3^- or 4^+, with the 3^- being favored.

The 5.6-MeV level of Pb^{208} was reported in an (α,α') experiment,[40] and given a tentative 3^- assignment. Our work agrees with this assignment.

The 6.2-MeV level has not been reported before. The only indication of a Pb^{208} level near this energy is in a $Pb^{206}(t,p)Pb^{208}$ experiment of Bjerregaard *et al.*,[43] where levels were seen at 6.11 and 6.20 MeV. They suggested that these came from 2-particle 2-hole excitations. This would not contradict our assignment of 2^+. Gillet *et al.*[6] predict a 2^+ level at 6.20 MeV. As discussed above, assignment of 0^+ cannot be ruled out. Since there are no known monopoles in nearby nuclei, nor any predicted, we make the assignment: $2^+(0^+)$.

A $T=1$ electric quadrupole state has been predicted[44] to lie above two oscillator shell energies, or above 12 MeV in Pb^{208}. No strong excitation was observed up to an excitation energy of 18.3 MeV, although there was a high sensitivity to $E2$ excitations as is evident in Fig. 2.

The vibrating-liquid-drop model was not tested as extensively on the other isotopes, but in no case was a marked divergence found. As we shall discuss later in the section on the weak-coupling model, the high degree of similarity in the extracted reduced nuclear transition probabilities is a strong test of the collectivity of these levels. Hence we might expect that the ρ_{tr} which fits one isotope, would fit them all.

Pb^{206} Levels

There are no published strengths for the excited collective states of Pb^{206}, except the recent (p,p') results from Saclay.[36] The 2.649-MeV (3^-) level has been identified as a singlet level. Cross sections for this level were more precise since this work on Pb^{206} did not begin until a year after the general experiment began. The stability and reproducibility of the data increased in that interval.

The 4.1- and 4.3-MeV levels of Pb^{206} were identified as 2^+ and 4^+, respectively. There was no sign of splitting of these levels, using a resolution of 200 keV. The $B(EL)$'s of these levels are nearly equal to those of the corresponding levels in Pb^{208}.

Pb^{207} Levels

The excitation of Pb^{207} at about 2.6 MeV ($L=3$) has been split in several experiments.[34,45] The energy difference between the two levels is about 39 keV. The single peak observed at our 200-keV resolution was analyzed as both a single level and as two levels

[38] V. Gillet, M. A. Melkanoff, and J. Ziegler (unpublished).
[39] J. LeTourneaux and J. M. Eisenberg, Nucl. Phys. **85**, 119 (1966).
[40] J. Alster, Phys. Rev. **141**, 1138 (1966).
[41] A. Scott and M. P. Fricke, Phys. Letters **20**, 654 (1966).
[42] T. H. Schucan, Nucl. Phys. **61**, 417 (1965); L. I. Schiff, Phys. Rev. **92**, 988 (1954).
[43] J. H. Bjerregaard, Ole Hansen, O. Nathan, and S. Hinds, Nucl. Phys. **89**, 337 (1966).
[44] B. R. Mottelson, in *Proceedings of the International Conference on Nuclear Structure*, edited by D. A. Bromley and E. W. Vogt (University of Toronto Press, Toronto, 1960), p. 539; S. Fallieros and R. A. Ferrell, Phys. Rev. **116**, 660 (1959).
[45] J. C. Hafele and R. Woods, Phys. Letters **23**, 579 (1966).

separated by 39 keV. Both techniques yielded the same summed cross sections (±1%). Because other techniques[45] can give better relative transition probabilities between the two peaks, we only quote the summed nuclear transition probability.

The 4.1-MeV ($L=2$) level has been split into a doublet[34] separated by 35 keV. The same general treatment as the above was used on this level. The 4.290-MeV ($L=4$) level has been seen only as a singlet.[34]

Bi^{209} Levels

The 2.6-MeV ($L=3$) "level" will be discussed in the next section. This "level" has recently been split into six levels:

2.489 $(\frac{3}{2}+)$
2.560 $(\frac{9}{2}+)$
2.580 $(\frac{7}{2}+)$
2.597 $(\frac{13}{2}$, $\frac{11}{2}+)$ } "lower" peak
2.615 $(\frac{5}{2}+)$
2.739 $(\frac{15}{2}+)$ } "upper" peak.

The level at 2.489 MeV contributes only 4% to the summed strength[45] and was omitted from the analysis. The summed "lower" peak could be partially separated from the 2.739-MeV peak when the energy resolution was reduced to 130 keV. The "upper" peak was usually poorly resolved, but the summation of both peaks was consistent with the GBROW curve of Fig. 15. As we show in the next section, the 2.489-MeV peak, which we omitted from our analysis, should contribute a strength of about $B(E3)=0.027e^2b^3$. When we add this to the experimentally determined values, we obtain a summed nuclear transition probability of $B(E3)=0.70e^2b^3$. This is in agreement with the Pb^{208} strength of $B(E3)=0.72e^2b^3$.

There have been no published reports of splitting of the 4-MeV levels in Bi^{209}. Our data show only a broad peak beginning at 3.9 MeV and continuing to 5 MeV. The total cross section of this hump was similar (±20%) to the summed cross sections of the Pb^{208} 2^+ and 4^+ levels.

C. Weak-Coupling Model

The weak-coupling model[10] predicts that the properties of collective states in odd-A nuclei can be determined by considering the weak coupling of the odd particle (or hole) to the vibrations of a neighboring even-even core. This weak coupling tends to split the even-even state into a multiplet. The number of states in this splitting is $2j_<+1$, where $j_<$ is the smaller of the particle (hole) or core spin. The sum of the strengths of the multiplet should equal that of the core state.

Recently Hafele has reported[45] the energy splitting of the octupole states in Pb^{207} and Bi^{209} in (p,p') experiments, in agreement with the weak-coupling model. The relative cross sections between the multiplets also agree well with the theory.

TABLE III. Strengths of octupole multiplets.

Isotope	Energy (MeV)	Spin/parity	Experimental relative strength[a] (%)	$B(E3)$ e^2b^3	Theoretical multiplet strength[a]
Bi^{209}	2.489	$\frac{3}{2}+$	4.1	0.027	0.039
	2.560	$\frac{9}{2}+$	15.1	0.102	0.097
	2.580	$\frac{7}{2}+$	12.7	0.086	0.078
	2.597	$\frac{13}{2}+$, $\frac{11}{2}+$	37.7	0.256	0.252
	2.615	$\frac{5}{2}+$	8.7	0.059	0.058
	2.739	$\frac{15}{2}+$	21.7	0.170	0.155
Pb^{207}	2.625	$\frac{5}{2}+$	43	0.271	0.271
	2.664	$\frac{7}{2}+$	57	0.359	0.359

[a] Reference 45.

Our experiment was of broad resolution (~200 keV) so that *summed* cross sections and reduced nuclear transition probabilities were obtained. These results may be combined with Hafele's work to produce $B(EL)$'s for each of the multiplets. The results are in Table III. As noted in Table II, the Bi^{209} octupole states were split into two groups in our experiment. The 2.489-MeV peak was not analyzed, and it was assumed that this level would have 4.1% of the total strength as determined by Hafele.

Table II shows that the sum of $B(EL)$'s of the multiplets of Pb^{207} and Bi^{209} equals that of their respective core states of Pb^{206} and Pb^{208} within experimental error. This conservation of strength as the number of nucleons changes is a primary indication of collectivity.

D. Dispersion Effects

The elastic scattering from the Pb isotopes was measured as an experimental check of the elastic scattering calculations[19] and parameters, and as a means of searching for higher-order effects in the scattering. In first-order treatments of elastic electron scattering, the nucleus usually is treated as a rigid body and the internal degrees of freedom are ignored. A higher-order process that may affect the elastic scattering is dynamic polarization or dispersive scattering in which the nucleus is first virtually excited by the electron, and then during a subsequent transition and scattering process, the excitation energy is returned to the same electron, thereby leaving the nucleus in the ground state.

In a preliminary report[12] a search for dispersion effects was undertaken by comparing elastic scattering from Pb^{207} to that of Pb^{208}. For the range of electron energies of this experiment, effects such as Coulomb distortion of the electron waves and radiative processes should be nearly the same for these nuclei but dispersive scattering may be different because of the different level structures. Evidence for dispersion effects might appear as a variation in ratios of the cross sections of

the isotopes as a function of electron energy. The ratios found were different from unity by a few percent, but uncertainties in target thickness precluded definitive conclusions about the presence of dispersion effects. Since agreement was found with the elastic-phase-shift calculations of Fischer and Rawitscher[19] with the usual corrections, it is unlikely that dispersion effects are large in this energy range.

We have repeated these measurements at 40, 50, 60, and 70 MeV at 130° with more carefully prepared targets (see Fig. 1) of Pb^{206}, Pb^{207}, and Pb^{208} of almost equal surface densities. Pb^{206} has a strong collective electric quadrupole level at 0.803 MeV which might give rise to enhanced dispersive scattering if an energy-weighted perturbation denominator enters into the formalism. After correcting for target thicknesses, recoil differences, etc.,[12] the cross-section ratios found were

$$\sigma_{206}/\sigma_{208}=1.001\pm0.046,$$
$$\sigma_{207}/\sigma_{208}=0.997\pm0.043.$$

The main source of error was in accurate determination of target thickness. Our procedures are discussed in detail in Ref. 23.

The conclusion arrived at is that *differences* in dispersion scattering of these isotopes must be less than 4.5% for the above experimental conditions.

V. CONCLUSIONS

This experiment shows that low-energy ($E_0\lesssim100$ MeV), high-resolution, inelastic electron scattering is valuable for the determination of multipolarity, $B(EL)$, and R_{tr} of collective excited electric multipole states. However, it is doubtful if the details of models may be checked with momentum transfers less than that required to reach the first diffraction minima. The need for high resolution, energy, and momentum transfer inelastic electron scattering is evident. Although this experiment has employed a numerical phase-shift analysis,[6,7] the use of the analytical Glauber theory[46,47] for forward angles and high energies seems to hold promise.

The striking similarity of the excitation energies, the reduced nuclear transition probabilities, $B(EL)$, and the transition radii R_{tr} for the corresponding levels studied in the four isotopes is a strong indication that these levels are similar and collective. The transition mechanism is unaffected by the addition or subtraction of one or two nucleons.

Since low-q electron scattering is model-dependent only to about $\pm2\%$ for these isotopes, it was possible to extract values of $B(EL)$ and R_{tr} with final accuracies of $\pm6\%$. This a marked improvement over other methods.

A renormalization of the experimental cross sections to an infinite energy so that data could be analyzed in Born-approximation may have merit.[48]

ACKNOWLEDGMENTS

The authors appreciate the over-all support given this project by the entire laboratory staff under Professor H. L. Schultz. We wish to thank the electron scattering group of C. K. Bockelman, T. H. Curtis, R. A. Eisenstein, and M. A. Duguay for collaborations on theory, equipment, and procedures, and E. Comeau and G. Cole for help in target fabrication and other aspects of the experiment. J. Berti, Miss K. Lappert, and Miss B. Grieb assisted in producing this paper. Many discussions and a great deal of help from Dr. L. E. Wright and Professor D. S. Onley with regard to the distorted-wave code are gratefully appreciated. We thank Dr. V. Gillet for his discussion and calculations relating to this work.

[46] R. J. Glauber, *Lectures in Theoretical Physics* (Interscience Publishers Inc., New York, 1959), Vol. I. p. 315.

[47] I. Zh. Petkov, V. K. Luk'yanov, and Yu. S. Pol, Yadern. Fiz. 4, 556 (1966) [English transl.: Soviet J. Nucl. Phys. 4, 395 (1967)].

[48] T. H. Schucan (private communications).